

Ordering kinetics of cylindrical and spherical microdomains in an SIS block copolymer by synchrotron SAXS and rheology

Jin Kon Kim^{*1}, Hee Hyun Lee¹, Moonhor Ree², Ki-Bong Lee^{3,4}, Yongjoon Park⁴

¹ Department of Chemical Engineering and Polymer Research Institute, Pohang University of Science and Technology, Pohang, Kyungbuk 790-784, Korea

² Department of Chemistry and Polymer Research Institute, Pohang University of Science and Technology, Pohang, Kyungbuk 790-784, Korea

³ Department of Physics, Pohang University of Science and Technology, Pohang, Kyungbuk 790-784, Korea

⁴ Pohang Accelerator Laboratory, Pohang University of Science and Technology, Pohang, Kyungbuk 790-784, Korea

(Received: July 18, 1997; revised manuscript of September 15, 1997)

SUMMARY: The ordering kinetics of cylindrical and spherical microdomains in a polystyrene-*block*-polyisoprene-*block*-polystyrene (SIS) copolymer were studied using synchrotron small-angle X-ray scattering (SAXS) and rheology upon quenching the sample from a disordered state to an ordered state having either spherical or cylindrical microdomains. The SIS exhibits an order to order transition at $\approx 181^\circ\text{C}$, a lattice disordering transition at $\approx 210^\circ\text{C}$ and becomes disordered at higher temperatures. Higher order peaks in the SAXS profiles corresponding to hexagonally packed cylindrical (HEX) microdomains appeared after less than 1 h when the sample was quenched from 235°C to 170°C . When quenched from 235°C to 200°C , a broad higher order peak at $\approx 1.65 q_m$, corresponding to spheres with *liquid-like* short-range order, was persistent up to 4 h before higher order peaks corresponding to body-centered cubic (BCC) microdomains appeared. We repeated this experiment by changing temperature from one ordered state with BCC microdomains to another with HEX microdomains, and vice versa. The BCC microdomains were attained within 1 h when heating from 170°C to 200°C . The transition between HEX and BCC is thermoreversible. The time evolution of dynamic storage modulus G' is in good agreement with that of SAXS intensity.

Introduction

Numerous studies have been reported on the order-disorder transition (ODT) in block copolymers during the past two decades^{1,2}. However, although the ordering process of microdomains in a block copolymer from a disordered state to ordered states has been studied very recently, the mechanism is not fully understood^{3–12}. Floudas et al.³ found that the ordering process of a polystyrene-*block*-polyisoprene (SI) copolymer can be described by an Avrami-type nucleation and growth mechanism, and this depended on the quenching depth (ΔT), namely, the distance between T_{ODT} and the phase-separating temperature. When ΔT is very small, the Avrami exponent is about 4, while it becomes 3 for larger ΔT . On the other hand, Takenaka et al.⁸ showed that, for very large ΔT , the ordering process is described by the spinodal decomposition mechanism, not by the nucleation and growth mechanism. Also, the ordering process depends upon the molecular architecture of block copolymers⁴.

Using small-angle X-ray scattering (SAXS) and rheology, Adams et al.¹¹ investigated the ordering kinetics of highly asymmetric SI and SIS copolymers with spherical microdomains of PS and reported that (i) the ordering kinetics of these copolymers is much slower than that observed for nearly symmetric SI copolymers with simi-

lar T_{ODT} ; and (ii) when the quenching depth is the same, the complete ordering of body-centered cubic (BCC) microdomains for a triblock copolymer takes much more time than for a diblock copolymer^{4,11}.

It has been recently found that some block copolymers have multiple ordered states, and the transition from one ordered state to another is referred to as an order to order transition (OOT)^{13–24}. Thus, it is very interesting to investigate the ordering process of a block copolymer with OOT when temperature is changed from one ordered state (e.g. cylindrical microdomains) to another (e.g. spherical microdomains). Very recently, Sakurai et al.²⁵ have studied the ordering kinetics from thermally frozen cylindrical microdomains to lamellar microdomains at equilibrium using temperature jumping experiment by synchrotron small-angle X-ray scattering (SAXS). Also, some research groups^{26,27} predicted theoretically an intermediate state when one microdomain is transformed into another. However, to our best knowledge, the ordering transition (or kinetics) of a block copolymer between spherical and cylindrical microdomains has not been studied experimentally.

In this study, using synchrotron SAXS and rheology, we investigated the ordering kinetics of cylindrical and spherical microdomains in a polystyrene-*block*-polyiso-

prene-*block*-polystyrene (SIS) copolymer upon quenching the sample from a disordered state to the ordered state having either spherical or cylindrical microdomains. This experiment was repeated by changing temperature from an ordered state with spherical microdomains to another with cylindrical microdomains, and vice versa.

Experimental part

Materials

A commercial grade (Vector 4111, Dow-Exxon Polymer Co.) SIS triblock copolymer was employed in this study. It has a weight-average molecular weight (M_w) of 1.427×10^5 , a weight fraction of the PS block of 0.183, and a polydispersity index of 1.09²⁴. Samples were prepared by first dissolving a predetermined amount of the block copolymer in toluene in the presence of an antioxidant (Irganox 1010; Ciba-Geigy Group) and then slowly evaporating the solvent. After completely removing traces of the solvent, the specimen was finally annealed at 140 °C for 48 h.

Rheological properties

Using an Advanced Rheometric Expansion System (ARES) with parallel plates of 25 mm diameter, dynamic temperature sweep experiment and temperature jumping tests were performed. Dynamic temperature sweep experiment was done under isochronal conditions with increasing temperature from 160 to 240 °C as well as decreasing temperature from 240 to 160 °C to investigate T_{OOT} and T_{ODT} . Also this temperature sweep was performed to confirm thermoreversibility of the transition between one ordered state and another with increasing temperature from 160 °C to 200 °C and annealing at 200 °C for 1 h, then decreasing the temperature from 200 °C to 140 °C. The heating and cooling rates of these experiments were 0.5 °C/min. The strain amplitude (γ_0) and the angular frequency (ω) were 0.03 and 0.05 rad/s, respectively. After a strain sweep at 160 °C, we found that a linear viscoelastic regime was obtained when γ_0 was less than 0.05 at this temperature. In order to measure the ordering kinetics of this SIS copolymer, the time evolutions of dynamic storage and loss moduli (G' and G'') were measured at $\omega = 0.05$ rad/s after temperature was changed from a disordered state to two ordered states, and from one ordered state to the other. The setting temperature was achieved less than 2 min in our rheometer when changing from initial temperature.

Synchrotron small angle X-ray scattering

Time-resolved SAXS experiments were conducted using the beam line (3C2) at the Pohang Light Source, Korea. SAXS profiles were measured continuously during the particular kinetic experiment with an exposure time of 10 s. But, for some specimens, the exposure time was increased to 30 s in order to detect more clearly the existence of higher order peaks. The incident beam was focused with a toroidal mirror and monochromatized using a double crystal Si(111) monochromator at a wavelength (λ) of 0.1598 nm, and scattered

intensity ($I(q)$) was detected by a diode-array position sensitive detector (ST-120; Princeton Instruments Inc.) allowing various wave vectors ($q = 4\pi \sin(\theta/2)/\lambda$ where θ is the scattered angle)²⁸. The sample was located in the heating block in a way that the film normal is parallel to the incident beam direction, and the film thickness was 1.8 mm. Two heating blocks were used for the temperature jumping experiment. The specimen soaked for certain times depending on initial temperature in the first heating block was pneumatically placed into the second heating block maintained at the setting temperature. After placing the sample into the second heating block, the specimen reached the setting temperature within 10 min, depending on the gap between initial and setting temperatures.

Results and discussion

Order-to-disorder and order-to-order transitions

Fig. 1 gives the temperature sweep of storage modulus G' at $\omega = 0.05$ rad/s and γ_0 of 0.03 during heating and cooling with a rate of 0.5 °C/min. It can be seen that, during heating, G' first decreases slowly with increasing temperature and reaches a minimum at ≈ 181 °C. Then, it increases and has a maximum at ≈ 190 °C. Finally it decreases again, first at a slow rate to 210 °C and then with much faster rate above 210 °C, which is consistent with results by Sakamoto et al.²⁴ The temperature at which a precipitous decrease in G' is observed is often

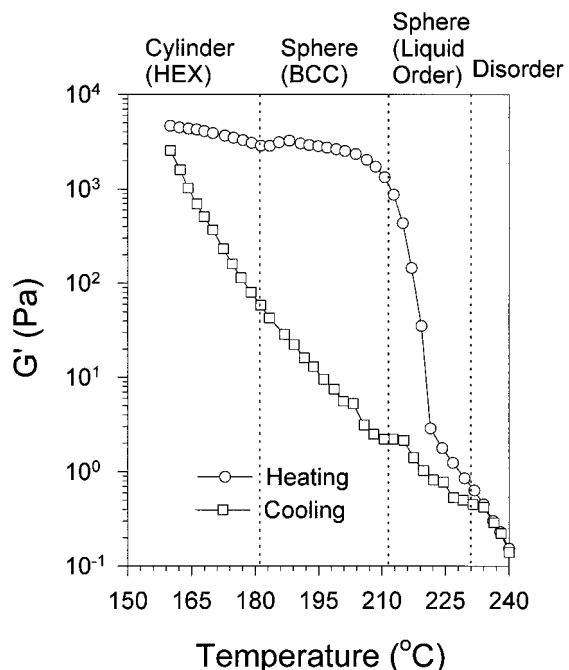


Fig. 1. Temperature sweep of G' at $\gamma_0 = 0.03$ and $\omega = 0.05$ rad/s during heating from 160 to 240 °C (○), and during cooling from 240 to 160 °C (□). The heating and cooling rates are 0.5 °C/min

referred to as the T_{ODT}^{29-32} . Using this definition, one can obtain a T_{ODT} of $\approx 210^\circ\text{C}$.

However, this definition must be reserved for highly asymmetric block copolymers^{2,23} since in these block copolymers spheres with *liquid-like* short-range order can be found at temperatures higher than the T_{ODT} defined above. Recently, Schwab and Stühn³³ showed that, for an asymmetric SI copolymer (volume fraction of PS is 0.11) spheres, with *liquid-like* order existed between BCC and homogeneously disordered state, which was deduced from the existence of high order peaks not corresponding to BCC microdomains in SAXS profiles. Thus, the above-mentioned rheological criterion²⁹⁻³² as the definition of T_{ODT} should be carefully employed for highly asymmetric block copolymers without SAXS profiles allowing one to determine whether higher order peak(s) corresponding to spheres with *liquid-like* short-range order exist or not. Otherwise, the temperature delineating spheres with *liquid-like* short-range order from BCC microdomain, namely the lattice disordering transition temperature (T_{LDT}), can be erroneously taken as the T_{ODT} . On the other hand, another rheological criterion, namely that the T_{ODT} is taken as the temperature above which plots of $\log G'$ versus $\log G''$ show temperature independence at lower frequencies, becomes powerful for determining the T_{ODT} of highly asymmetric block copolymers^{2,24}. When this criterion is employed, the T_{ODT} of the block copolymer employed in this study was determined to be $\approx 230^\circ\text{C}$ ^a.

Therefore, the temperature of $\approx 210^\circ\text{C}$ in Fig. 1 would correspond to T_{LDT} and not to T_{ODT} . This will be elaborated later when SAXS profiles are present. The increase in G' near at 185°C with increasing temperature is due to the formation of a new type of microdomain. According to ref.²⁴, this block copolymer has a cylindrical microdomain at temperatures less than 181°C , but a spherical microdomain at temperatures above 181°C , verified by transmission electron microscopy (TEM).

It can be also seen in Fig. 1 that, during cooling, the increase in G' with decreasing temperature is rather gradual, and there is no sharp increase in G' . This result suggests that, for a highly asymmetric block copolymer, the ordering of the microdomain during cooling process from a disordered state to an ordered state is very slow compared with the disordering of the microdomain during heating process from the ordered state to the disordered state. Therefore, the temperature sweep of G' during heating is more powerful to detect the transition temperature, which was already demonstrated by many research groups²⁹⁻³². Based on Fig. 1, one can distinguish 4 differ-

ent regimes for this block copolymer; (1) the ordered state with cylindrical microdomains below $\approx 181^\circ\text{C}$; (2) the body-centered cubic spherical (BCC) microdomains with *solid-like* long-range order between ≈ 181 and $\approx 210^\circ\text{C}$; (3) spheres with *liquid-like* short-range order between ≈ 210 and $\approx 230^\circ\text{C}$; and (4) a disordered state at higher temperatures, although these regimes are not delineated very accurately.

Ordering kinetics of spherical microdomains from disordered state

Fig. 2 gives the time evolution of overall SAXS profiles and SAXS profiles near the first order peak after quenching to 200°C (an ordered state with BCC microdomains at equilibrium) from 235°C after soaking the specimen for 10 min at 235°C . Here, overall SAXS profiles in Fig. 2(a) are arbitrarily shifted to avoid overlaps. The two SAXS profiles at 200°C and 235°C obtained during heating were given in dotted curves for comparison. In Fig. 2, the time zero is taken as the time when the temperature at the specimen first reached 200°C . Although polyisoprene can degrade at higher temperatures for longer times³⁴, we checked by GPC that no degradation of this block copolymer occurred within this time period. This is because the nitrogen environment and an antioxidant were used in addition to short time exposure at 235°C (e.g. ≈ 10 min).

It can be seen in Fig. 2(a) that the maximum scattering intensity (I_m) grows with time, but there exists a broad higher order peak. However, as we examine closely the SAXS profiles, the peak maximum appears at $\approx 1.65 q_m$, which does not correspond to $\sqrt{2} q_m$ nor $\sqrt{3} q_m$, where q_m is the maximum peak position. These SAXS profiles are different from the SAXS profile (curve II) at 200°C obtained during heating where $\sqrt{2} q_m$ and $\sqrt{3} q_m$ are clearly seen. When a block copolymer shows SAXS profiles with diffraction peaks appearing at the ratios of $1:\sqrt{2}:\sqrt{3}:\sqrt{4} \dots$ in reciprocal space, it has BCC microdomains, while it has hexagonally packed cylindrical (HEX) microdomains when diffraction peaks appear at $1:\sqrt{3}:\sqrt{4}:\sqrt{7} \dots$ in reciprocal space.

The higher order peak occurring at $\approx 1.65 q_m$ was also seen at time zero (curve (1) in Fig. 2(a)). But, since it took ≈ 10 min to reach 200°C when quenched from 235°C , some morphological change might happen during this time. This broad higher order peak appearing in Fig. 2(a) was also reported by Adams et al.¹¹ for a highly asymmetric SIS copolymer. However, they ascribed it to the vitrification of large-amplitude composition fluctuation existing in a disordered state, although the prediction

^a Very recently, Sakamoto et al. (*Macromolecules* **30**, 5321 (1997)) showed that the T_{ODT} of Vector 4111 was estimated to be $\approx 270^\circ\text{C}$ by extrapolation of experimentally determined T_{ODT} of Vector 4111/dioctyl phthalate mixtures based on a dilution theory. Thus, the reported value of the T_{ODT} ($\approx 230^\circ\text{C}$) for Vector 4111 in this study might not be quite accurate. However, this change in T_{ODT} does not affect any conclusion in this paper on the ordering kinetics between HEX and BCC microdomains.

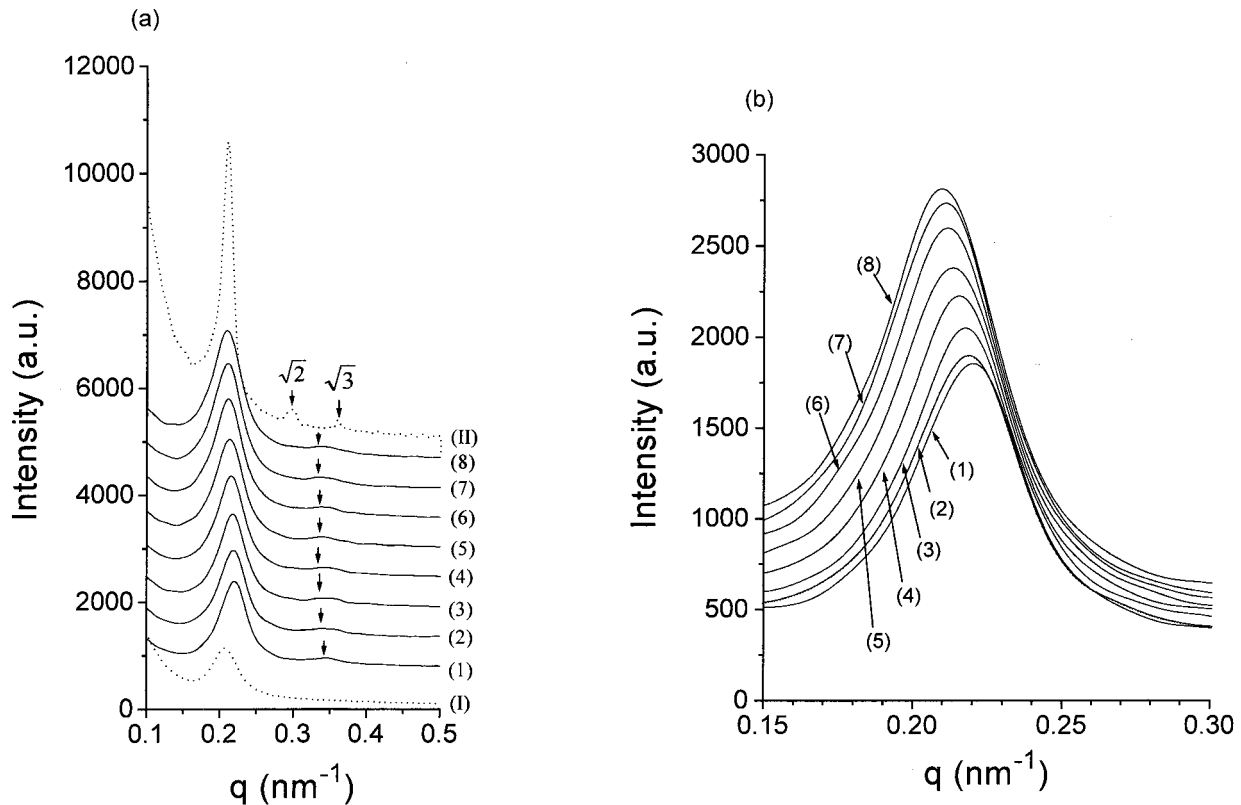


Fig. 2. (a) Overall SAXS profiles and (b) SAXS profiles near the first order peak as a function of time when quenching to 200 °C from 235 °C after soaking for 10 min at 235 °C: (1) 0 s; (2) 650 s; (3) 1294 s; (4) 2746 s; (5) 4696 s; (6) 5286 s; (7) 6230 s; and (8) 6748 s. Time zero is taken as the time when the specimen temperature first reaches 200 °C. Dotted curves (I) and (II) in part (a) are SAXS profiles obtained at 235 °C and 200 °C, respectively, during heating. All curves in part (a) are arbitrarily shifted to avoid overlaps

based on a model corresponding to spheres with *liquid-like* short-range order (or hard spheres) gives a higher order peak occurring at $\approx 1.68 q_m$ in the SAXS profile (see Fig. 13 in ref.¹¹), while the random phase approximation (RPA) model with the concentration fluctuation effect does not predict the existence of the higher order peak. However, Sakamoto et al.²⁴) showed that there existed a higher order peak located between $\sqrt{2} q_m$ and $\sqrt{3} q_m$ in SAXS profiles at 212 °C during heating of the same SIS block copolymer employed in this study, and that this peak resulted from the existence of spheres with *liquid-like* short-range order. Therefore, from the existence of the higher order peak shown in Fig. 2(a), we can conclude that BCC microdomains with *solid-like* long-range order were not attained up to ≈ 2 h at 200 °C when quenched from 235 °C.

It is noted that our synchrotron SAXS experiment was done up to ≈ 2 h due to the limit of beam time allocation, and long-time ordering kinetics of this block copolymer was not studied in-situ using synchrotron SAXS experiment. In order to carry out a long-time ordering experiment, the specimen was prepared by first quenching to

200 °C from 235 °C after soaking at 235 °C for 10 min, then annealing at 200 °C for four different times, 0.5, 2, 4, and 6 h, respectively, in a heating block under nitrogen environment, and finally quenching into ice water to fix the morphology. The SAXS experiment for these samples was done at room temperature with a longer exposure time of 30 s to investigate higher order peaks more clearly. Although the morphology of a block copolymer observed during an in-situ annealing test might be different from that obtained from the above method owing to a possible morphological change during quenching, we assume these are almost the same, since microdomains are sufficiently fixed during quenching. The SAXS profiles for these samples annealed at four different times are given in Fig. 3. It can be seen that (i) a broad higher order peak, not corresponding to $\sqrt{2}$ nor $\sqrt{3} q_m$, was observed for the samples annealed up to 2 h, (ii) a peak occurring near $\sqrt{2} q_m$ was found for the sample annealed for 4 h, and (iii) higher order peaks corresponding to $\sqrt{2}$ and $\sqrt{3} q_m$ were clearly visible for the sample annealed for 6 h. Therefore, we conclude that, when the sample is quenched from 235 °C to 200 °C, spheres with *liquid-like*

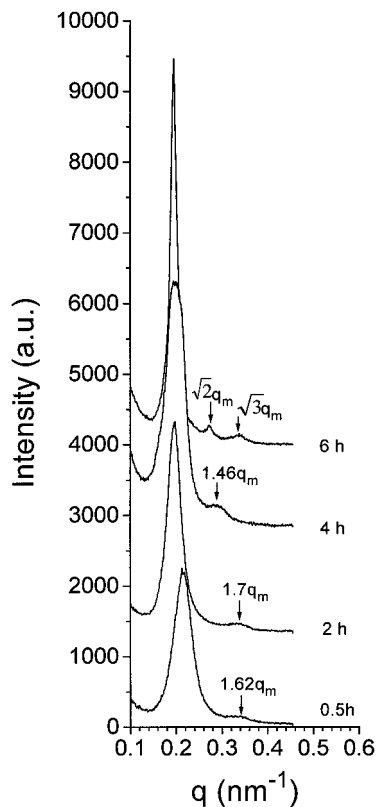


Fig. 3. Overall SAXS profiles of the specimens prepared by first quenching to 200°C from 235°C after soaking for 10 min at 235°C, then annealing at 200°C for various times (h)

short-range order persist up to ≈ 2 h, while BCC microdomains with *solid-like* long-range order might be attained at ≈ 6 h. At 4 h annealing, some ordering in BCC as well as spheres with *liquid-like* short-range order may coexist, although the former seems to dominate over the latter.

The time evolutions of I_m , q_m , and the half width at half maximum intensity, σ_q , are given in Fig. 4. Open symbols were taken from results in Fig. 3. It is worth noting in Fig. 4 that (i) I_m increases steadily with time; (ii) q_m decreases steadily with time up to 2 h and then seems to level off; (iii) σ_q is almost constant until 4 h, but it decreases significantly between 4 h and 6 h. These results also suggest that BCC microdomains with *solid-like* long-range order were not fully attained up to 4 h.

Fig. 5 gives the time evolutions of G' and G'' at 200°C after quenching from 235°C. It can be seen that G' and G'' do not change within 1 h and increase rapidly with time between 1 h and 3 h, and then seem to reach a steady value at times greater than 4 h. Initial increase in G' and G'' at time zero is attributed to the fact that G' and G'' at 200°C are larger than those at 235°C. The values of G' and G'' at time zero are slightly larger than those obtained during cooling (see Fig. 1). However, the value of G' after 6 h given in Fig. 5 is less than that at 200°C during heating, as given in Fig. 1. This suggests that BCC micro-

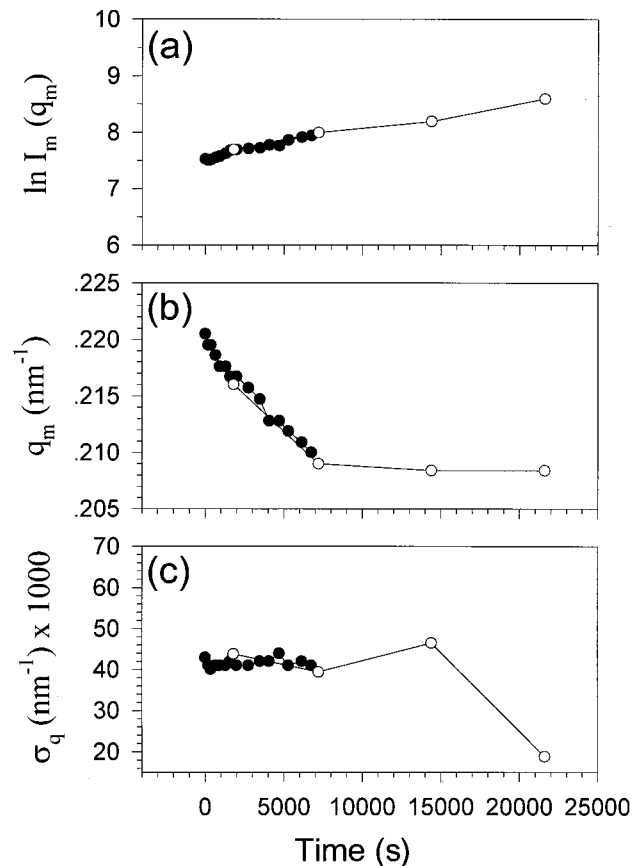


Fig. 4. Time evolutions of (a) I_m , (b) q_m , and (c) σ_q when jumping to 200°C from 235°C after soaking for 10 min at 235°C

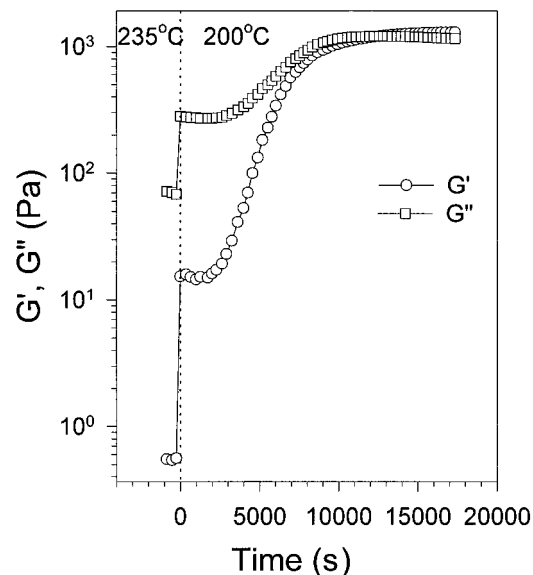


Fig. 5. Time evolutions of G' (\circ) and G'' (\square) at $\gamma_0 = 0.03$ and $\omega = 0.05$ rad/s when quenching to 200°C from 235°C after soaking for 10 min at 235°C

domains with *solid-like* long-range order (or an equilibrium state) can be attained at very long time (say ≈ 6 h or even longer), which is an agreement with results given

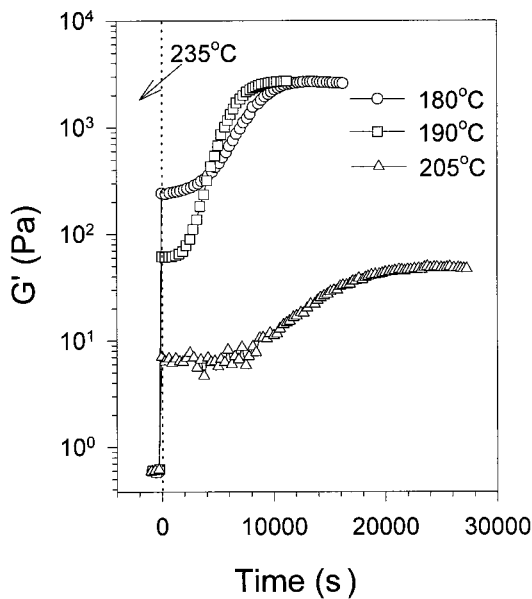


Fig. 6. Time evolution of G' at $\gamma_0 = 0.03$ and $\omega = 0.05$ rad/s when quenching from 235°C to various temperatures: (Δ) 205°C , (\square) 190°C , and (\circ) 180°C after soaking for 10 min at 235°C

by Adams et al.¹¹, who showed that for an asymmetric SIS triblock copolymer, G' reached a steady value after ≈ 20 h when the ordering temperature is just 35°C lower than T_{ODT} . This slow ordering is attributed to the fact that, when quenched from a disordered state, BCC microdomains with *solid-like* long-range order could be attained only after crossing over the state consisting of spheres with *liquid-like* short-range order. The ordering in spheres with *liquid-like* short-range order should not be confused with the thermal concentration fluctuation found sometimes in a disordered state. If this block copolymer had been in a disordered state at 200°C with the thermal concentration fluctuation, the values of G' and G'' would not have increased with time.

Fig. 6 shows that with increasing the quench depth, the starting time for the increase in G' , namely the incubation time, becomes shorter. For instance, when temperature is decreased to 190°C from 235°C , G' keeps the initial value until 0.5 h, and the value is larger than that obtained during cooling given in Fig. 1. Then, G' starts to increase very rapidly up to 2 h, and finally reaches a steady value which is essentially the same as the G' at 190°C during heating as given in Fig. 1. However, the incubation time

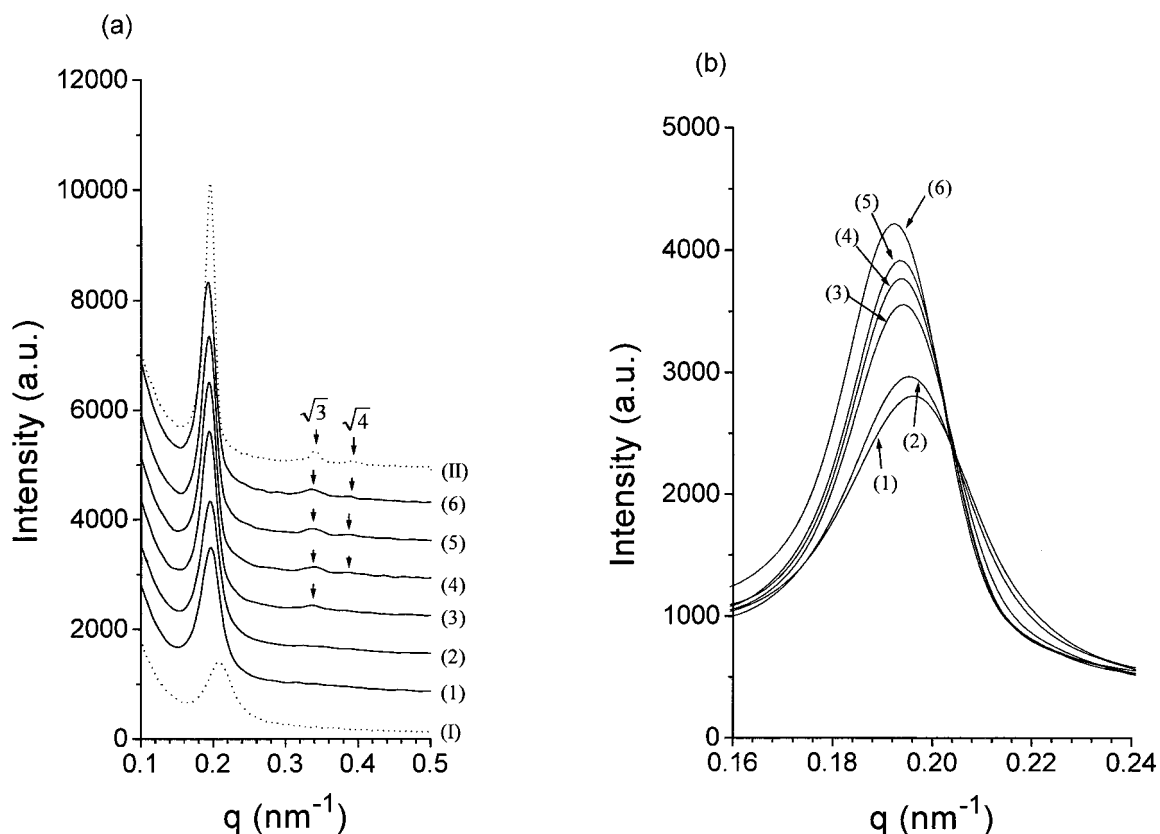


Fig. 7. (a) Overall SAXS profiles and (b) SAXS profiles near the first order peak as a function of time when quenching to 170°C from 235°C after soaking for 10 min at 235°C : (1) 0 s; (2) 228 s; (3) 752 s; (4) 1368 s; (5) 1608 s; and (6) 2818 s. Time zero is taken as the time when the specimen temperature first reaches 170°C . Dotted curves (I) and (II) in part (a) are SAXS profiles obtained at 235°C and 170°C , respectively, during heating. All curves in part (a) are arbitrarily shifted to avoid overlaps

is not proportionally decreased to the quenching depth if the OOT took place in this region. For instance, the incubation time when quenched to 180°C is about twice that when quenched to 190°C, although the quenching depth of the former is 10°C larger than that of the latter.

Ordering kinetics of cylindrical microdomains from disordered state

Fig. 7 gives the time evolutions of overall SAXS profiles and SAXS profiles near the first order peak after quenching to 170°C (an ordered state with cylindrical microdomains) from 235°C after soaking for 10 min at 235°C. The two SAXS profiles at 170°C and 235°C obtained during heating are given in dotted curves for comparison. Here, time zero is taken as the time when the temperature at the specimen first reached 170°C. It can be seen in Fig. 7 that the maximum intensity grows very rapidly between 228 s and 752 s and a peak corresponding to $\sqrt{3} q_m$ first appears after 752 s, which indicates that the block copolymer attained HEX microdomains after this time. It took very short time to develop HEX microdomains when quenched from a disordered state, which is quite different from the ordering of BCC microdomains given

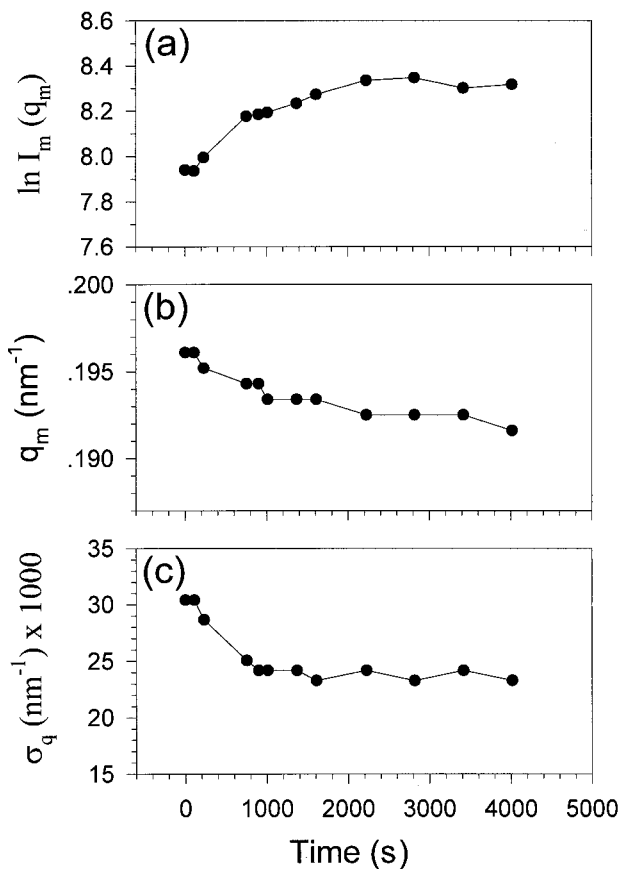


Fig. 8. Time evolutions of (a) I_m , (b) q_m , and (c) σ_q when quenching to 170°C from 235°C after soaking for 10 min at 235°C

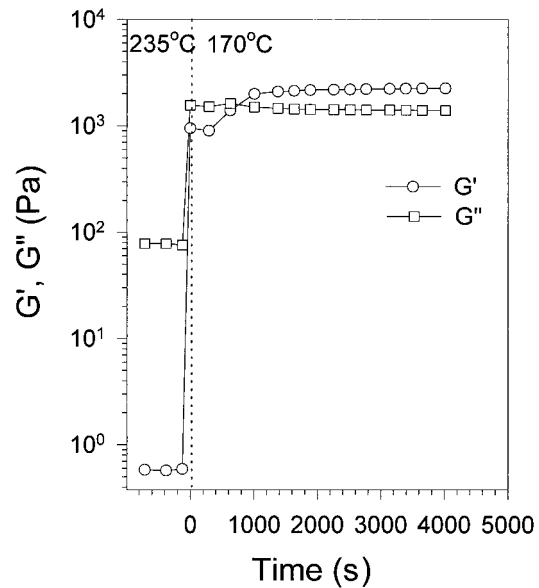


Fig. 9. Time evolutions of G' (○) and G'' (◻) at $\gamma_0 = 0.03$ and $\omega = 0.05$ rad/s when quenching to 170°C from 235°C after soaking for 10 min at 235°C

in Fig. 2. This is due to the difference in quenching depth as well as the difference in ordering formation of microdomain structures (HEX versus BCC).

The time evolutions of I_m , q_m , and σ_q are given in Fig. 8. It can be noted in Fig. 8 that until 1000 s, I_m increases exponentially with time, while q_m and σ_q decrease steadily with time. Then, all of these leveled off after 1000 s, implying that HEX microdomains are completely attained within 20 min.

Fig. 9 gives the time evolutions of G' and G'' at 170°C after quenching from 235°C. It can be seen that G' changed very rapidly with time until 1000 s and leveled off, which is consistent with SAXS results in Fig. 8. It should be mentioned that Winter et al.³⁵ reported that the first order peak of SAXS profiles is sensitive to the order of the microdomain scale, while rheological properties are sensitive to the micron-scale grain structure, namely, the degree of continuity of the PS cylinders across the domain boundary. This suggests that it be not necessary to have the same results for SAXS and rheology. However, Balsara et al.³⁶ and Hashimoto et al.¹⁰ showed that the grain size has only little effect on the elastic modulus. Therefore, the good agreement between the experimental results from SAXS and rheology (Fig. 8 and 9) implies that the higher ordering of HEX microdomains for this SIS block copolymer was attained easily.

Ordering kinetics of spherical microdomains from cylindrical microdomains

Fig. 10 gives the change in overall SAXS profiles and SAXS profiles near the first order peak with time when

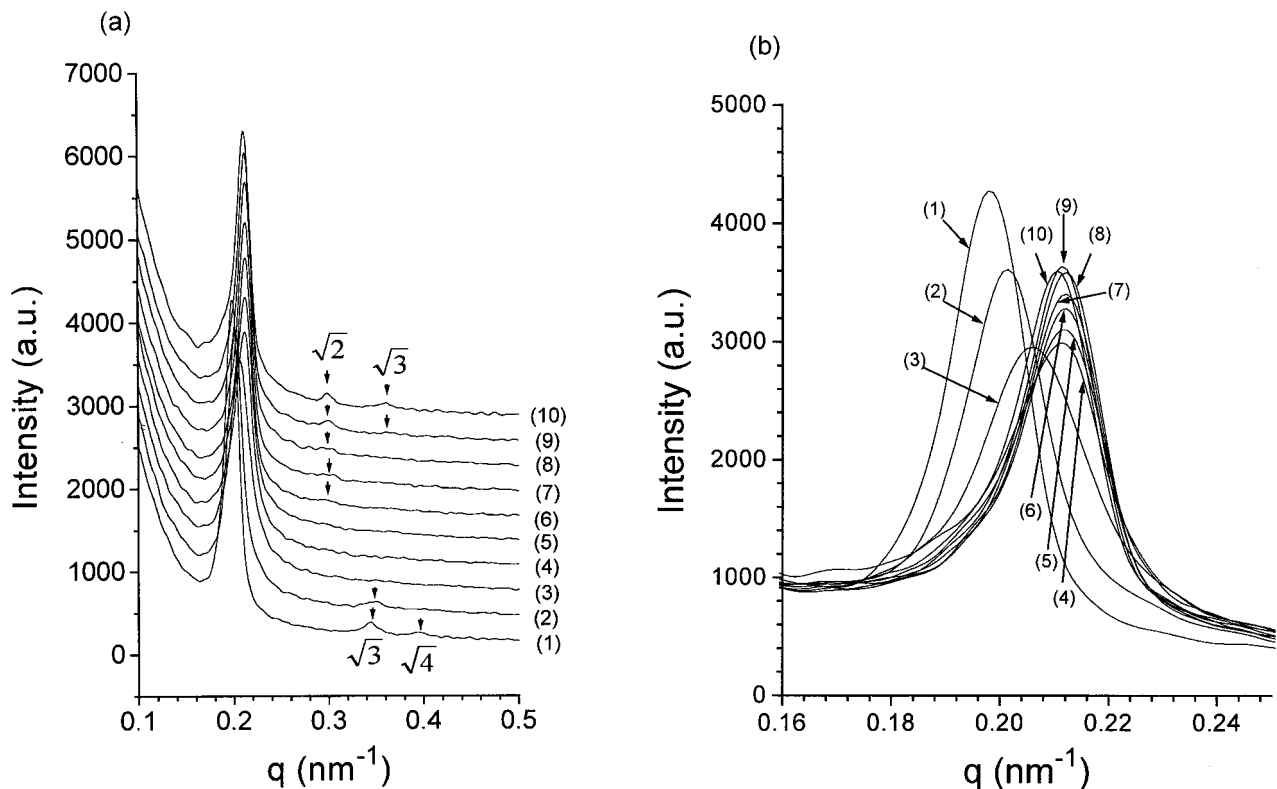


Fig. 10. (a) Overall SAXS profiles and (b) SAXS profiles near the first order peak as a function of time when heating to 200 °C from 170 °C after soaking for 50 min at 170 °C: (1) 60 s (194 °C); (2) 132 s (196 °C); (3) 192 s (199 °C); (4) 250 s (200 °C); (5) 312 s; (6) 496 s; (7) 662 s; (8) 850 s; (9) 1588 s; and (10) 2852 s. The time zero is taken as the time when the specimen at one heating block was first placed into the other heating block maintained at 200 °C. All curves in part (a) are arbitrarily shifted to avoid overlaps

temperature is increased to 200 °C from 170 °C after specimen was soaked for 50 min at 170 °C. It took about 200 s to reach 200 °C in the jumping experiment of SAXS. It can be found that until 132 s, the higher order peaks at $\sqrt{3} q_m$ and $\sqrt{4} q_m$ corresponding to the HEX microdomains remained, and that the higher order peaks at $\sqrt{2} q_m$ and $\sqrt{3} q_m$ corresponding to the BCC microdomains occurred after 500 s. This is quite different from the ordering process of BCC microdomains when quenched from a disordered state, at which higher order peaks at $\sqrt{2} q_m$ and $\sqrt{3} q_m$ cannot be seen even after 7200 s. This leads us to consider that the ordering of BCC microdomains took place more easily during heating compared with cooling.

The time evolutions of I_m , q_m , and σ_q are given in Fig. 11. It can be seen that before reaching 200 °C, the peak intensity decreased dramatically with time, while q_m increases rapidly from 0.198 nm⁻¹ to 0.212 nm⁻¹ at short times. Once the temperature at the specimen reaches 200 °C, q_m does not further change with time, while I_m increases exponentially with time until 1000 s and then levels off, suggesting that the ordering of BCC microdomains may be completed within 1000 s. It is worth noting in Fig. 11 that σ_q exhibited a maximum near at 200 s,

implying that this state might be an intermediate state between HEX and BCC, but not a disordered state, since I_m has a relatively large value. However, we could not conclude whether or not this intermediate state corresponds to an equilibrium morphology, although recent theories^{26,27} suggest this possibility. This will be studied in detail in the near future. Nevertheless, according to results given in Fig. 11, we conclude that the transition of HEX microdomains into BCC microdomains occurred without a complete dissolution of HEX microdomains into a disordered state.

From the q_m , the interdomain spacing between HEX microdomains (D_{HEX}) was calculated to be 31.4 nm at 170 °C and the interdomain spacing between BCC microdomains (D_{BCC}) to be 28.6 nm at 200 °C. Note that $D_{\text{HEX}} = \sqrt{(4/3)} d_{100}$ and $D_{\text{BCC}} = \sqrt{(3/2)} d_{110}$, respectively, where d_{100} and d_{110} are defined by $2\pi/q_m$. Thus, the difference between D_{HEX} and D_{BCC} is less than 10%. When HEX microdomains are transformed into BCC microdomains, with keeping the same interdomain spacing in addition to the same volume fraction of PS block, the radius (R_{HEX}) of a HEX microdomain must be smaller than that (R_{BCC}) of a BCC microdomain. This is attributed to the fact that the cylindrical axis of HEX microdomains undulates and

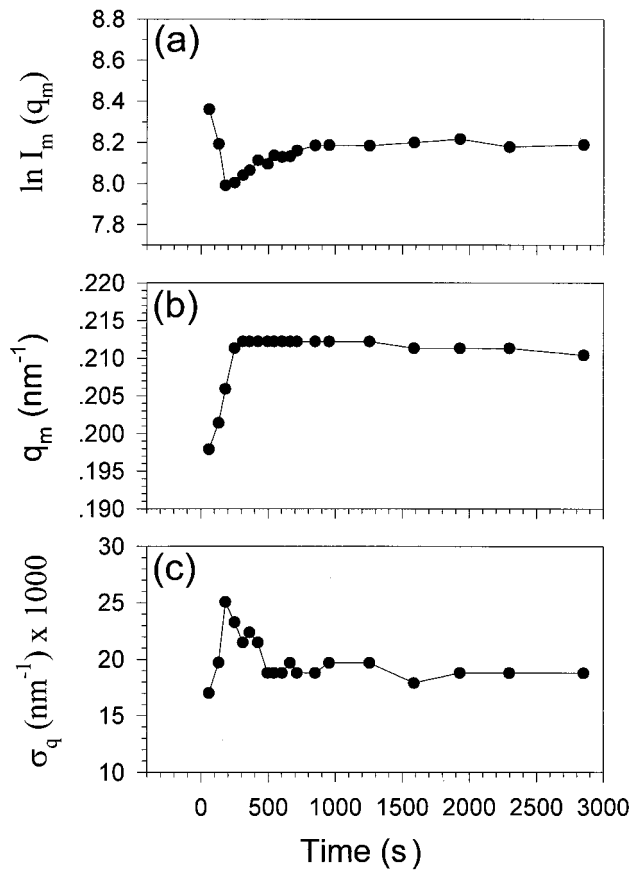


Fig. 11. Time evolutions of (a) I_m , (b) q_m , and (c) σ_q when heating to 200°C from 170°C after soaking for 50 min at 170°C

is broken into BCC spheres²³). This undulation is also theoretically predicted by Qi and Wang²⁶) and by Laradji et al.²⁷) On the basis of the scattering theory, $R_{\text{HEX}}/R_{\text{BCC}}$ is given by:

$$\frac{R_{\text{HEX}}}{R_{\text{BCC}}} = \frac{d_{100}}{d_{110}} \left(\frac{64\phi}{27\sqrt{3}\pi} \right)^{1/6} \quad (1)$$

For this block copolymer with ϕ for PS block of 0.15, this ratio is obtained to be 0.72.

The time evolution of G' is shown in Fig. 12 when temperature is rapidly increased to 200°C from 170°C after specimen was soaked for 2 h at 170°C. The specimen temperature reached 200°C within 2 min in our rheometer after jumping, and the fluctuation in temperature was within 5°C before it is stabilized. It is rather interesting to see in Fig. 12 that initially G' drops significantly, then increases rapidly and finally reaches a steady value after 5000 s. It is noted that the drop in G' found in Fig. 12 is more evident if compared with that observed at $\approx T_{\text{OOT}}$ during heating given in Fig. 1. We also observed this kind of a drop in G' before increasing and leveling off when temperature is increased to 190°C from 170°C for this block copolymer. However, when polystyrene or

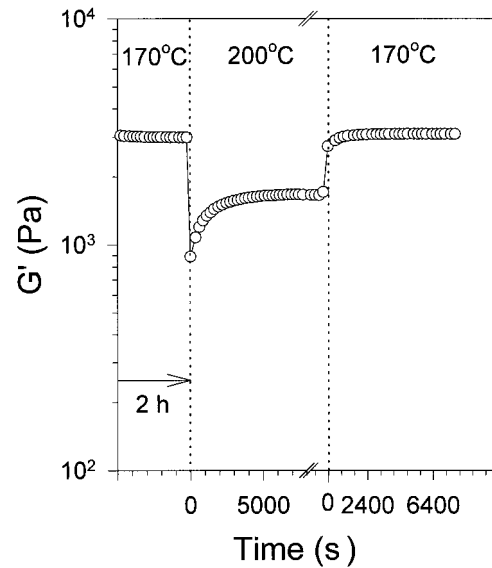


Fig. 12. Time evolution of G' (\circ) at $\gamma_0 = 0.03$ and $\omega = 0.05$ rad/s when the specimen was rapidly heated to 200°C from 170°C after soaking at 170°C for 2 h, and when quenched to 170°C from 200°C

polyisoprene homopolymer is rapidly heated from 170°C to 200°C (or 190°C), we could not observe this drop in G' . Therefore, the drop in G' shown in Fig. 12 is not due to a temperature fluctuation before stabilizing the setting temperature in this rheometer, rather it can be explained as follows.

When the specimen is rapidly heated from 170°C to 200°C, we speculate that at short times microdomains may take a superheated state of undulated cylinders formed near T_{OOT} ($\approx 181^\circ\text{C}$). The value of G' for this block copolymer with a superheated state of undulated cylinders at 200°C is expected to be lower than that at T_{OOT} , since this temperature is $\approx 20^\circ\text{C}$ higher than the T_{OOT} . With increasing time the undulated cylindrical microdomains with superheated state are gradually transformed into BCC microdomains with *solid-like* long-range orders, thus G' increases accordingly. However, the steady value of G' at 200°C is less than that at 170°C.

It should be mentioned that during the transition from HEX microdomains into BCC microdomains, a plateau (or an incubation) in G' does not appear before G' increases and levels off with annealing time. This behavior is different from the case when quenched from a disordered state to 200°C at which a plateau (or an incubation) in G' was visible up to 1 h before G' increases and levels off with annealing time (see Fig. 5). Also, there is no higher order peak at $\approx 1.65 q_m$ in the SAXS profile as shown in Fig. 10. It is noted that this higher order peak was found when quenched from a disordered state to 200°C (see Fig. 2). These results lead us to conclude that, when the specimen was rapidly heated from 170°C to 200°C, there is no need to cross over spheres with *liquid-*

like short-range order before transforming into BCC microdomains with *solid-like* long-range order, which suggests that a complete dissolution of HEX microdomains into a disordered state is not necessary during the transition from HEX to BCC microdomains. Therefore, the minimum in G' observed at $\approx T_{OOT}$ shown in Fig. 1 is not due to a complete dissolution of HEX microdomains into a disordered state, but due to the undulated cylindrical microdomains formed at $\approx T_{OOT}$ from HEX microdomains.

Using theories^{37,38)} available at the present time, we now test whether or not a complete dissolution of HEX microdomains into a disordered state can take place before being transformed into BCC microdomains. This is simply checked because the free energy barrier between the HEX microdomain and the disordered state can be theoretically compared with that between HEX and BCC microdomains. According to Leibler's theory³⁷⁾ extended by Mayes and Olvera de la Cruz³⁸⁾, the free energy difference for a triblock copolymer between HEX microdomains and the disordered state $((\Delta F)_3)$, and that between BCC microdomains and the disordered state $((\Delta F)_6)$, are given by:

$$\frac{(\Delta F)_n}{\rho_0 k_B T} = -\frac{27a_n^4(1 + \gamma_n)^3(3\gamma_n - 1)}{(64)^2(\beta_n)^3} \quad (n = 3 \text{ and } n = 6) \quad (2a)$$

where

$$\gamma_n = \left[1 + \frac{64\beta_n(\chi - \chi_s)N}{9a_n^2} \right]^{1/2} \quad (n = 3 \text{ and } n = 6) \quad (2b)$$

where ρ_0 is the density of monomer unit, k_B is the Boltzmann constant, T is the absolute temperature, χ and χ_s are Flory's interaction parameters at the pre-set temperature and at the spinodal temperature, respectively, and N is the total number of statistical segments (or degrees of polymerization). The coefficients of a_n and β_n given in refs.³⁶⁾ and³⁷⁾ depend on the volume fraction but not on temperature. It should be mentioned that different expressions of χ and N give different values of $(\Delta F)_3$ and $(\Delta F)_6$. Among many expressions of $\chi_{PS/PI}$ available at the present time, in this study we choose the following expression³⁹⁾:

$$\chi = -0.0419 + 38.54/T \quad (3)$$

Also, N and the volume fraction of PS (f) are obtained by:

$$N = (v_{s,PS} M_w,PS + v_{s,PI} M_w,PI) / V_{ref} \quad (4a)$$

$$f = v_{s,PS} M_w,PS / (v_{s,PS} M_w,PS + v_{s,PI} M_w,PI) \quad (4b)$$

where $v_{s,i}$ is the specific volume of block i ($i = PS$ and PI) given in ref.²⁾, $M_{w,i}$ is the weight-average molecular

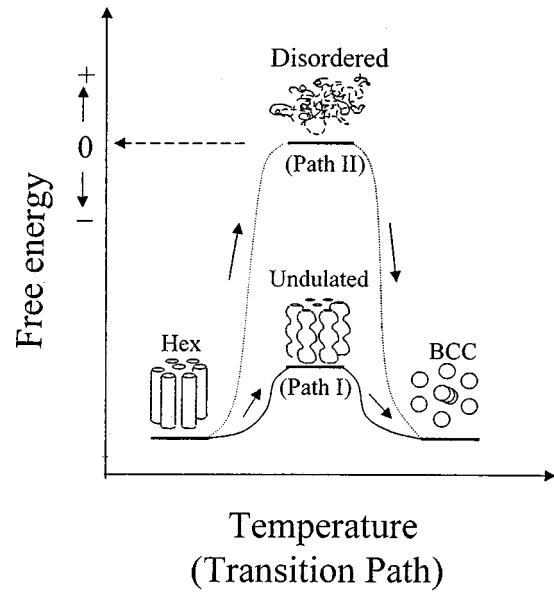


Fig. 13. Schematic of morphological transformation from HEX to BCC microdomains

weight of block i , and V_{ref} is taken as the monomeric volume of PS and becomes $1/\rho_0$ in Eq. (2).

We found from the calculation based on Eqs. (2)–(4) that the predicted T_{OOT} is 180.7°C , which is very close to experimental data, while the predicted T_{ODT} is 195.3°C , which is lower than the experimental data. When temperature is increased from 180°C to 185°C , the value of $(\Delta F)_3N/(k_B T)$ was increased from -0.01626 to -0.008030 , while the value of $(\Delta F)_6N/(k_B T)$ was increased from -0.01619 to -0.009193 . This suggests that BCC microdomains are more stable than HEX microdomains at temperatures greater than T_{OOT} , while HEX microdomains are more stable at temperatures less than T_{OOT} . Also, it is found that at temperatures slightly greater than T_{OOT} the free energy barrier for a transition of a HEX microdomain into a disordered state (i. e., $-(\Delta F)_3/(\rho_0 k_B T)$) is much larger than that of the HEX microdomain into the BCC microdomain (i. e., $(F_3 - F_6)/(\rho_0 k_B T)$). For instance, at 185°C , the former was 0.008030 , which is about 7 times the latter (0.001163). Based on the above analysis, the transition from HEX to BCC microdomains can be schematically shown in Fig. 13. Among these two possible paths, path (I) is more likely to be the true path, although the exact mechanism will only be investigated in detail in the near future.

Ordering kinetics of cylindrical microdomains from spherical microdomains

Fig. 14 gives the time evolutions of overall SAXS profiles and SAXS profiles near the first order peak when temperature is decreased to 170°C from 200°C after spe-

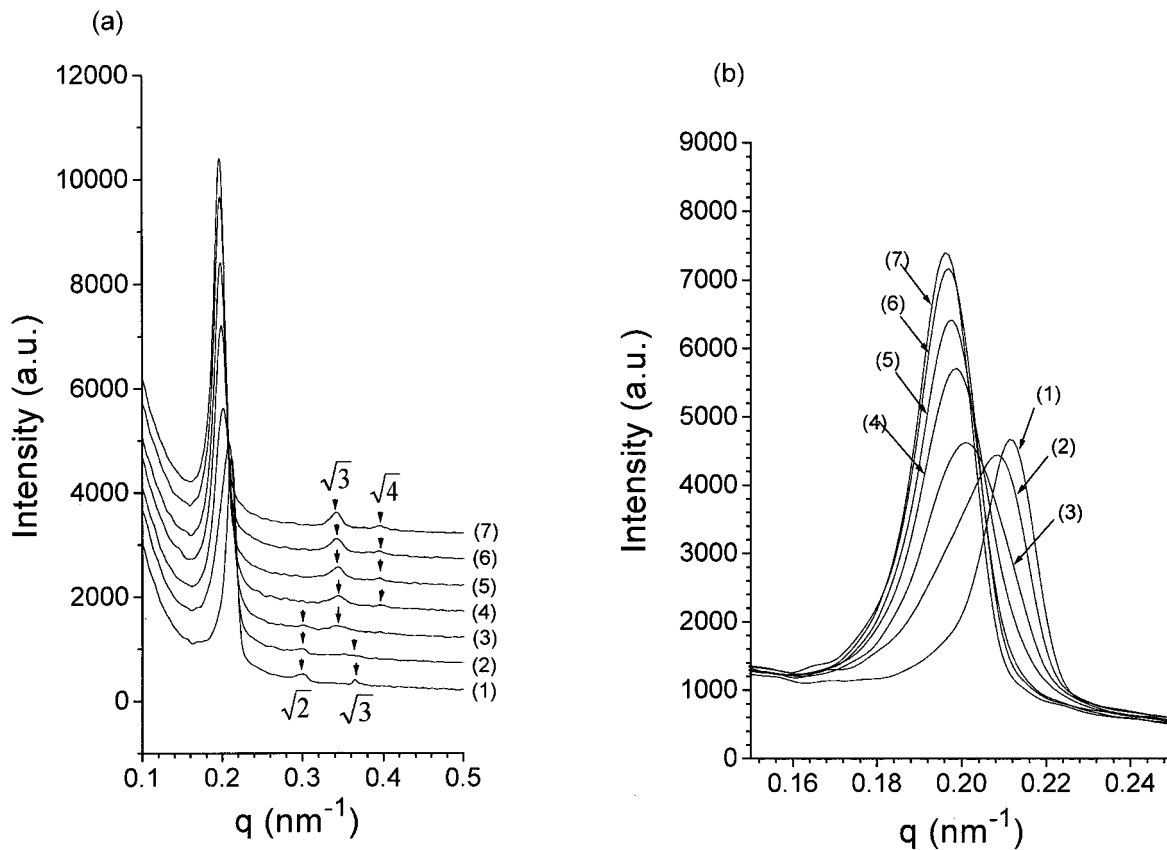


Fig. 14. (a) Overall SAXS profiles and (b) SAXS profiles near the first order peak as a function of time when quenching to 170 °C from 200 °C after soaking at 200 °C for 110 min: (1) 60 s (190 °C); (2) 408 s (170.3 °C); (3) 528 s (169.7 °C); (4) 640 s (170 °C); 822 s; (6) 1080 s; and (7) 2386 s. The time zero is taken as the time when the specimen at one heating block was placed into the other heating block maintained at 170 °C. All curves in part (a) are arbitrarily shifted to avoid overlaps

cimen was soaked for 110 min at 200 °C. It took about 400 s to reach 170 °C when quenching from 200 °C in our SAXS experiment. It can be seen that, until the temperature at the specimen reaches 170 °C, BCC microdomains are persisting. However, as soon as temperature reaches 170 °C, BCC microdomains are transformed very quickly into HEX microdomains.

The time evolutions of I_m , q_m , and σ_q are given in Fig. 15. It can be seen that before reaching 170 °C, peak intensity decreases slowly with time, and q_m also decreases from 0.21 nm⁻¹ to 0.196 nm⁻¹ with time. Once the temperature of the specimen is maintained at 170 °C, q_m does not further change with time, while I_m increases exponentially with time until 1000 s and then levels off. But, σ_q exhibited a maximum near at 500 s, meaning that this state might be an intermediate state between BCC and HEX microdomains.

The time evolution of G' is also shown in Fig. 12 when temperature is decreased to 170 °C from 200 °C. It can be seen that the increment in G' occurred at very short times without showing any drop in G' and that the steady value is exactly the same as that treated at 170 °C for 2 h. Very recently, Laradji et al.²⁷⁾ theoretically predicted that the

transition from HEX into BCC proceeds directly, while the transition from BCC into HEX proceeds through an intermediate state. Thus, they concluded these two transitions are not thermoreversible. However, as shown in Fig. 16, we consider that the transition between HEX and BCC for this block copolymer is thermoreversible except that the T_{OOT} (or the minimum in G') obtained during the cooling cycle is 15 °C less than that obtained during the heating cycle. This is also consistent with results in Fig. 12.

Conclusions

In this study, we have investigated the ordering kinetics of cylindrical and spherical microdomains in a polystyrene-*block*-polyisoprene-*block*-polystyrene (SIS) copolymer after quenching from the disordered state to an ordered state having either spherical or cylindrical microdomain, and from one of the ordered states to the other, using synchrotron SAXS and rheology. The SIS has an order to order transition at ≈ 181 °C, a lattice disordering above ≈ 210 °C, and reaches the disordered state at higher temperatures.

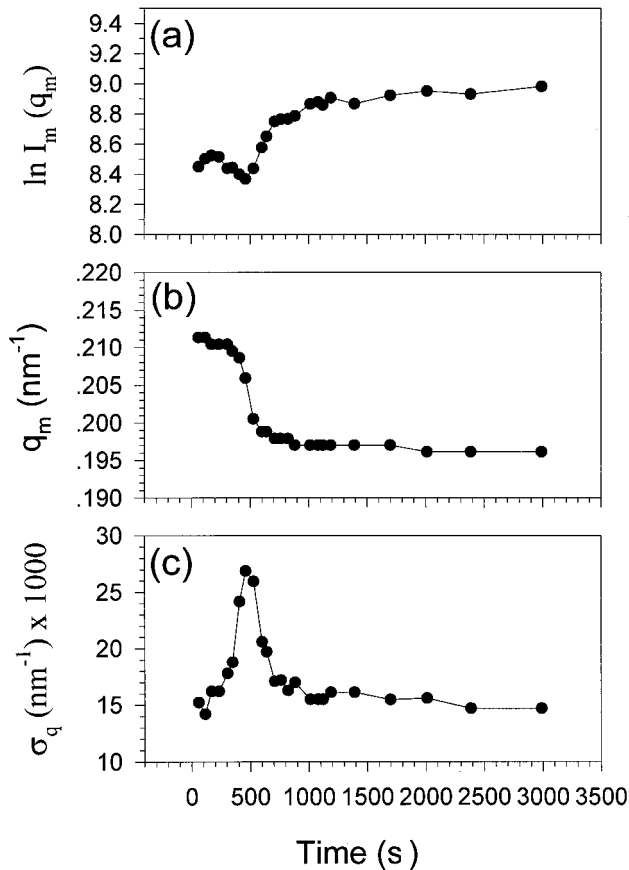


Fig. 15. Time evolutions of (a) I_m , (b) q_m , and (c) σ_q when quenching to 170°C from 200°C after soaking at 200°C for 110 min

Higher order peaks in the SAXS profile corresponding to the hexagonally packed cylindrical (HEX) microdomains appeared after less than 1 h when quenched from 235°C to 170°C. But, when quenched from 235°C to 200°C, it was found that (i) a broad higher order peak at $\approx 1.65 q_m$, corresponding to spheres with *liquid-like* short-range order, was persistent up to 4 h before higher order peaks corresponding to the body-centered cubic (BCC) microdomains appeared; and (ii) G' and G'' did not change within 1 h but increased rapidly with time between 1 h and 3 h, and then reached steady values at times greater than 4 h. The time evolution of G' is in good agreement with that of SAXS profiles. These results lead us to conclude that BCC microdomains with *solid-like* long-range order were not fully attained up to 4 h.

However, when heated to 200°C from 170°C, higher order peaks in the SAXS profile, corresponding to BCC microdomains, appeared within 1 h, without exhibiting a broad higher order peak at $\approx 1.65 q_m$. It was also found that the plateau in G' did not appear before G' increased and leveled off with annealing time. These results suggest that, during the transition from HEX to BCC microdomains, there is no need to cross over spheres with *liquid-*

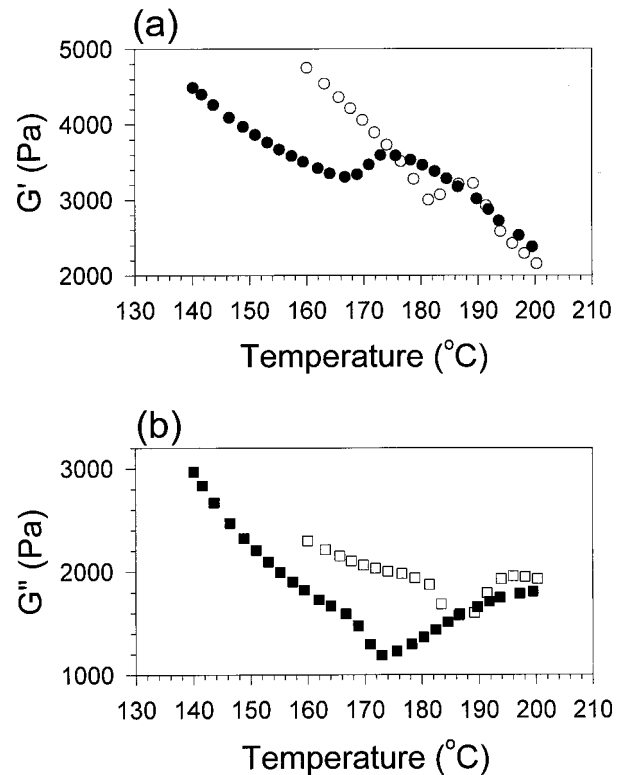


Fig. 16. Temperature sweep of (a) G' (○) and (b) G'' (◻) when first heating from 160 to 200°C (open symbols) and annealing at 200°C for 1 h, then cooling from 200 to 140°C (closed symbols)

like short-range order before transforming into BCC microdomains with *solid-like* long-range order. Therefore, the minimum in G' observed at $\approx T_{OOT}$ in the temperature sweep during heating is not due to a complete dissolution of HEX microdomains into a disordered state, but due to the undulated cylindrical microdomains formed at $\approx T_{OOT}$ from HEX microdomains. This is also theoretically confirmed based on the result that the free energy barrier between the HEX microdomain and the disordered state is larger than that between HEX and BCC microdomains near T_{OOT} . It is highly expected that undulated cylinders (or an intermediate state) be experimentally detected by transmission electron microscopy (TEM). This will be the subject of future investigations.

The transition between HEX and BCC was found to be thermoreversible except that the T_{OOT} (or the minimum point in G') obtained during cooling is 15°C less than that obtained during heating.

Acknowledgement: We acknowledge Prof. S. Sakurai at Kyoto Institute of Technology for reading this paper critically and sending ref.¹⁶⁾ This work was supported by *Korean Foundation and Science and Engineering* (# 94-0503-02-3). Synchrotron SAXS experiment at the PLS were supported by *Ministry of Science and Technology* (MOST) and *Pohang Iron & Steel Co.* (POSCO).

- ¹⁾ F. S. Bates, G. H. Fredrickson, *Annu. Rev. Phys. Chem.* **41**, 525 (1990)
- ²⁾ C. D. Han, D. M. Baek, J. K. Kim, T. Ogawa, T. Hashimoto, *Macromolecules* **28**, 5043 (1995)
- ³⁾ G. Floudas, N. Hadjichristidis, H. Iatrou, T. Pakula, E. W. Fischer, *Macromolecules* **27**, 7735 (1994)
- ⁴⁾ G. Floudas, S. Pispas, N. Hadjichristidis, T. Pakula, I. Erukhimovich, *Macromolecules* **27**, 7735 (1996)
- ⁵⁾ T. Hashimoto, *Macromolecules* **20**, 465 (1987)
- ⁶⁾ B. Stühn, A. Vilesov, H. G. Zachmann, *Macromolecules* **27**, 3560 (1994)
- ⁷⁾ J. G. Connell, R. W. Richards, *Prog. Colloid Polym. Sci.* **80**, 180 (1989); *Polymer* **32**, 2033 (1991)
- ⁸⁾ M. Takenaka, J. Linliu, Q. Ying, B. Chu, D. Peiffer, *Macromolecules* **28**, 2700 (1995)
- ⁹⁾ T. Hashimoto, N. Sakamoto, *Macromolecules* **28**, 4779 (1995)
- ¹⁰⁾ T. Hashimoto, T. Ogawa, N. Sakamoto, M. Ichimiya, J. K. Kim, C. D. Han, *Polymer* **39**, 1573 (1998)
- ¹¹⁾ J. L. Adams, D. J. Quiram, W. W. Graessley, R. A. Register, G. R. Marchand, *Macromolecules* **29**, 2929 (1996)
- ¹²⁾ D. Perahia, G. Vacca, S. S. Patel, H. J. Dai, N. P. Balsara, *Macromolecules* **27**, 7645 (1994)
- ¹³⁾ N. P. Balsara, H. J. Dai, H. Watanabe, T. Sato, K. Osaki, *Macromolecules* **29**, 3507 (1996)
- ¹⁴⁾ S. Sakurai, T. Momii, K. Taie, M. Shibayama, S. Nomura, T. Hashimoto, *Macromolecules* **26**, 458 (1993)
- ¹⁵⁾ S. Sakurai, H. Kawada, T. Hashimoto, L. J. Fetters, *Macromolecules* **26**, 5796 (1993)
- ¹⁶⁾ S. Sakurai, H. Kawada, T. Hashimoto, L. J. Fetters, *Proc. Jpn. Acad.* **69B**, 13 (1993)
- ¹⁷⁾ K. Almdal, K. A. Koppi, F. S. Bates, K. Mortensen, *Macromolecules* **25**, 1743 (1992)
- ¹⁸⁾ I. W. Hamley, K. A. Koppi, J. H. Rosedale, F. S. Bates, K. Almdal, K. Mortensen, *Macromolecules* **26**, 5959 (1993)
- ¹⁹⁾ S. Förster, A. K. Khandpur, J. Zhao, F. S. Bates, I. W. Hamley, A. J. Ryan, W. Bras, *Macromolecules* **27**, 6922 (1994)
- ²⁰⁾ K. A. Koppi, M. Tirrell, F. S. Bates, K. Almdal, K. Mortensen, *J. Rheol.* **38**, 999 (1994)
- ²¹⁾ D. A. Hajduk, S. M. Gruner, P. Rangarajan, R. A. Register, L. J. Fetters, C. Honecker, R. J. Albalak, E. L. Thomas, *Macromolecules* **26**, 490 (1994)
- ²²⁾ A. K. Khandpur, S. Förster, F. S. Bates, I. W. Hamley, A. J. Ryan, W. Bras, K. Almdal, K. Mortensen, *Macromolecules* **28**, 8796 (1995)
- ²³⁾ S. Sakurai, T. Hashimoto, L. J. Fetters, *Macromolecules* **29**, 740 (1996)
- ²⁴⁾ N. Sakamoto, T. Hashimoto, C. D. Han, D. Kim, N. Y. Vaidya, *Macromolecules* **30**, 1621 (1997)
- ²⁵⁾ S. Sakurai, H. Umeda, K. Taie, S. Nomura, *J. Chem. Phys.* **105**, 8902 (1996)
- ²⁶⁾ S. Qi, Z. G. Wang, *Phys. Rev. Lett.* **76**, 1679 (1996); *Phys. Rev. E* **55**, 1682 (1997)
- ²⁷⁾ M. Laradji, A. C. Shi, J. Noolandi, R. C. Desai, *Phys. Rev. Lett.* **78**, 2577 (1997); *Macromolecules* **30**, 3242 (1997)
- ²⁸⁾ B. J. Park, S. Y. Rah, Y. J. Park, K. B. Lee, *Rev. Sci. Instrum.* **66**, 1722 (1995)
- ²⁹⁾ F. S. Bates, *Macromolecules* **17**, 2607 (1984)
- ³⁰⁾ J. H. Rosedale, F. S. Bates, *Macromolecules* **23**, 2329 (1990)
- ³¹⁾ F. S. Bates, J. H. Rosedale, G. H. Fredrickson, *J. Chem. Phys.* **92**, 6255 (1990)
- ³²⁾ J. L. Adams, W. W. Graessley, G. R. Marchand, *Macromolecules* **27**, 6026 (1994)
- ³³⁾ M. Schwab, B. Stühn, *Phys. Rev. Lett.* **76**, 924 (1996)
- ³⁴⁾ J. H. Han, D. Feng, C. Choi-Feng, C. D. Han, *Polymer* **36**, 155 (1995)
- ³⁵⁾ H. H. Winter, D. B. Scott, W. Gronski, S. Okamoto, T. Hashimoto, *Macromolecules* **26**, 7236 (1993)
- ³⁶⁾ N. P. Balsara, H. J. Dai, H. Watanabe, T. Sato, K. Osaki, *Macromolecules* **29**, 3507 (1996)
- ³⁷⁾ L. Leibler, *Macromolecules* **13**, 1602 (1980)
- ³⁸⁾ A. M. Mayes, M. Olvera de la Cruz, *J. Chem. Phys.* **91**, 7228 (1991)
- ³⁹⁾ T. Hashimoto, Y. Ijichi, L. J. Fetters, *J. Chem. Phys.* **89**, 2463 (1988)